

Renormalization of NN Interaction with Lorentz-invariant Chiral Two Pion Exchange.

R. Higa,^{1,2,*} M. Pavón Valderrama,^{3,4,†} and E. Ruiz Arriola^{3,‡}

¹ *Universität Bonn, HISKP (Theorie), Nussallee 14-16, 53115 Bonn, Germany*

² *Jefferson Laboratory, 12000 Jefferson Avenue, Newport News, VA 23606 USA*

³ *Departamento de Física Atómica, Molecular y Nuclear,
Universidad de Granada, E-18071 Granada, Spain.*

⁴ *The H. Niewodniczański Institute of Nuclear Physics, PL-31342 Kraków, Poland*

(Dated: November 24, 2018)

The renormalization of the NN interaction with the Chiral Two Pion Exchange Potential computed using Lorentz-invariant baryon chiral perturbation theory is considered. The short distance singularity reduces the number of counter-terms to about a half as those in the heavy baryon expansion. Phase shifts and deuteron properties are evaluated and a general overall agreement is observed.

PACS numbers: 03.65.Nk,11.10.Gh,13.75.Cs,21.30.Fe,21.45.+v

Keywords: NN interaction, Two Pion Exchange, Renormalization, Relativity

I. INTRODUCTION

At long distances the Nucleon-Nucleon (NN) interaction can be written as (see e.g. [1] for a review)

$$\mathbf{V}(r) = \mathbf{V}_{1\pi}(r) + \mathbf{V}_{2\pi}(r) + \dots \quad (1)$$

where, $\mathbf{V}_{1\pi}(r)$ and $\mathbf{V}_{2\pi}(r)$ represent the One Pion Exchange (OPE) and the Two Pion Exchange (TPE) contributions to the potential, respectively. Up to power corrections in the distance r , one has $\mathbf{V}_{n\pi}(r) = \mathcal{O}(e^{-nm_\pi r})$. Such an expansion makes sense, since there is a clear scale separation at long distances. Actually, the omitted terms in Eq. (1) represent contributions whose ranges are shorter than $1/(2m_\pi) \sim 0.7\text{fm}$. These include three and higher pion exchanges, correlated meson exchanges, etc [2]. In momentum space, the expansion of Eq. (1) parallels an expansion on leading low momentum singularities, rather than a naive low momentum expansion. The systematic and model independent determination of those potentials was suggested several years ago [3, 4, 5, 6] and pursued by many others [7, 8, 9, 10, 11] (for some reviews emphasizing different viewpoints see e.g. [12, 13, 14, 15, 16] and references therein). However, in any scheme the potentials in Eq. (1) become singular at short distances, so one must truncate or renormalize the potential in a physically meaningful way in order to predict finite and unique phase shifts and deuteron properties. This has been a subject of much debate and controversy in recent times and we refer the interested reader to the literature for further details [10, 17, 18, 19, 20, 21, 22, 23, 24, 25, 26, 27, 28, 29, 30, 31].

In previous works by two of us (MPV and ERA) [25, 26, 28, 29] the renormalization of NN potentials was studied using chiral potentials based on the heavy baryon

formalism (HB- χ PT) [8, 10]. In the present paper, we extend those ideas to the case where Lorentz-invariant chiral potentials are used instead. In this case, the relativistic framework of baryon chiral perturbation theory (RB- χ PT) proposed by Becher and Leutwyler [32, 33] is employed in the construction of the two-pion exchange (TPE) component of the NN interaction. The remarkable difference between HB- and RB-TPE potentials lies on the long distance behavior [34, 35, 36, 37], due to the analytic structure of the πN scattering amplitude in the low energy region where the Mandelstam variable t is close to $4m_\pi^2$, m_π being the pion mass. Actually, one appealing feature of the RB-TPE potentials is that the long-distance two pion effects are correctly described, so that important contributions at the exponential level $\sim e^{-2m_\pi r}$ are properly re-summed, unlike its heavy baryon counterpart. In this work we are also interested on its different short distance behavior, which plays an important role on the renormalization program of the NN interaction developed in Refs. [25, 26, 28, 29]. We disregard, however, explicit Δ 's (see e.g. [38]) and other intermediate state contributions, assuming that those degrees of freedom have been integrated out.

As we have already mentioned, the calculation of scattering and bound state properties requires specifying the NN potential at short distances, which turns out to be highly singular for the Lorentz-invariant case. Actually, a crucial issue in the present context regards the number of necessary counter-terms required by the renormalizability of the S-matrix. In the single channel situation, the results found in Refs. [25, 26, 28, 29] in configuration space can be summarized as follows. If the potential is a regular one, i.e., $r^2|U(r)| < \infty$, there is freedom to choose between the regular and irregular solution of the corresponding Schrödinger equation. In the first case the scattering length is predicted, while in the second case the scattering length becomes an input of the calculation. Singular potentials fulfill $r^2|U(r)| \rightarrow \infty$ and do not allow this choice. For repulsive singular potentials [$r^2U(r) \rightarrow \infty$] the scattering length is *predicted* while for

*Electronic address: higa@itkp.uni-bonn.de

†Electronic address: mpavon@ugr.es

‡Electronic address: earriola@ugr.es

TABLE I: Sets of chiral coefficients considered in this work.

Set	Source	$c_1(\text{GeV}^{-1})$	$c_3(\text{GeV}^{-1})$	$c_4(\text{GeV}^{-1})$
Set I	πN [41]	-0.81	-4.69	3.40
Set II	NN [10]	-0.76	-5.08	4.70
Set III	NN [42]	-0.81	-3.40	3.40
Set IV	NN [20]	-0.81	-3.20	5.40
Set η	This work	-0.81	-3.80	4.50

attractive singular potentials [$r^2 U(r) \rightarrow -\infty$] the scattering length *must* be given. The case $r^2 U(r) \rightarrow g$ is very special and, for $g < -1/4$, yields ultraviolet limit-cycles [22, 39, 40]. For coupled channels one must diagonalize first the coupled channel potentials and apply the single channel rules to the outgoing eigenpotentials.

In order to avoid any possible misunderstanding we hasten to emphasize that our use of the word relativistic is in a narrow sense; we are only disregarding a naive heavy baryon expansion of the virtual nucleon states in the calculation of the potential and hence taking into account important anomalous thresholds singularities [32, 33]. This is *not the same* as providing a fully relativistic quantum field theoretical solution to the two-body problem by say, solving a Bethe-Salpeter equation or any two body relativistic equation. This has always been a problem rooted in the non-perturbative divorce between crossing and unitarity in few body calculations for which the present paper has nothing to say.

The paper is organized as follows. In Sec. II we give an overview of our formalism already used in Ref. [25, 26, 28, 29]. The key aspects on the derivation of the Lorentz-invariant TPE potential are briefly mentioned and the main differences with respect to the heavy baryon formalism are highlighted in Sec. III. The deuteron bound state is discussed in Sec. IV. Our predictions for phase shifts are displayed in Sec. V. Finally, in Sec. VI we draw our conclusions.

II. FORMALISM

Along the lines of Ref. [25, 26, 28, 29] we solve the coupled channel Schrödinger equation in configuration space for the relative motion, which in compact notation reads

$$-\mathbf{u}''(r) + \left[\mathbf{U}(r) + \frac{\mathbf{l}^2}{r^2} \right] \mathbf{u}(r) = k^2 \mathbf{u}(r). \quad (2)$$

The coupled channel matrix reduced potential is defined as usual, $\mathbf{U}(r) = 2\mu_{np}\mathbf{V}(r)$, where $\mu_{np} = M_p M_n / (M_p + M_n)$ is the reduced proton-neutron mass. For $j > 0$,

$\mathbf{U}(r)$ can be written as

$$\mathbf{U}^{0j}(r) = U_{jj}^{0j}, \quad (3)$$

$$\mathbf{U}^{1j}(r) = \begin{pmatrix} U_{j-1,j-1}^{1j}(r) & 0 & U_{j-1,j+1}^{1j}(r) \\ 0 & U_{jj}^{1j}(r) & 0 \\ U_{j-1,j+1}^{1j}(r) & 0 & U_{j+1,j+1}^{1j}(r) \end{pmatrix}.$$

In Eq. (2) $\mathbf{l}^2 = \text{diag}(l_1(l_1+1), \dots, l_N(l_N+1))$ is the angular momentum, $\mathbf{u}(r)$ is the reduced matrix wave function and k the C.M. momentum. In our case, $N = 1$ for the spin singlet channel ($l = j$) and $N = 3$ for the spin triplet channel, with $l_1 = j-1$, $l_2 = j$ and $l_3 = j+1$. The potentials used in this paper were obtained in Refs. [34, 35, 36], in coordinate space. We outline the main issues of this potential in Sec. III.

A. Long distance behaviour

At long distances, we assume the usual asymptotic normalization condition

$$\mathbf{u}(r) \rightarrow \hat{\mathbf{h}}^{(-)}(r) - \hat{\mathbf{h}}^{(+)}(r)\mathbf{S}, \quad (4)$$

with \mathbf{S} the coupled channel unitary S-matrix. The corresponding outgoing and incoming free spherical waves are given by

$$\hat{\mathbf{h}}^{(\pm)}(r) = \text{diag}(\hat{h}_{l_1}^{\pm}(kr), \dots, \hat{h}_{l_N}^{\pm}(kr)), \quad (5)$$

with $\hat{h}_l^{\pm}(x)$ the reduced Hankel functions of order l , $\hat{h}_l^{\pm}(x) = xH_{l+1/2}^{\pm}(x)$ ($\hat{h}_0^{\pm}(x) = e^{\pm ix}$), and satisfy the free Schrödinger's equation for a free particle.

The spin singlet state ($s = 0$) is an un-coupled state

$$S_{jj}^{0j} = e^{2i\delta_j^{0j}}, \quad (6)$$

while the spin triplet state ($s = 1$) comprises one un-coupled $l = j$ state

$$S_{jj}^{1j} = e^{2i\delta_j^{1j}}, \quad (7)$$

and the two channel coupled $l, l' = j \pm 1$ states for which we use Stapp-Ypsilantis-Metropolis (SYM or Nuclear bar) [45] parameterization

$$S^{1j} = \begin{pmatrix} S_{j-1,j-1}^{1j} & S_{j-1,j+1}^{1j} \\ S_{j+1,j-1}^{1j} & S_{j+1,j+1}^{1j} \end{pmatrix} = \begin{pmatrix} \cos(2\bar{\epsilon}_j) e^{2i\bar{\delta}_{j-1}^{1j}} & i \sin(2\bar{\epsilon}_j) e^{i(\bar{\delta}_{j-1}^{1j} + \bar{\delta}_{j+1}^{1j})} \\ i \sin(2\bar{\epsilon}_j) e^{i(\bar{\delta}_{j-1}^{1j} + \bar{\delta}_{j+1}^{1j})} & \cos(2\bar{\epsilon}_j) e^{2i\bar{\delta}_{j+1}^{1j}} \end{pmatrix}$$

In the present paper zero energy scattering parameters play an essential role, since they are often used (see below) as input parameters in the calculation of phase

TABLE II: The number of independent parameters (counter-terms) for the Lorentz-invariant baryon expansion potential (RB) different orders of approximation of the heavy baryon expansion (HB) potential. The scattering lengths are in fm^{*l+l'+1*} and are taken from NijmII and Reid93 potentials [43] in Ref. [44]. We use the (SYM-nuclear bar) convention, Eq. (11). The stars (*) mean that the behaviour is very dependent on the chosen set of chiral couplings.

Wave	α NijmII (Reid93)	OPE	HB-NLO	HB-NNLO Set I, II & III	HB-NNLO SetIV	RB-TPE
¹ <i>S</i> ₀	-23.727(-23.735)	Input	Input	Input	Input	Input
³ <i>P</i> ₀	-2.468(-2.469)	Input	—	Input	—	—(*)
¹ <i>P</i> ₁	2.797(2.736)	—	—	Input	—	—
³ <i>P</i> ₁	1.529(1.530)	—	Input	Input	Input	Input
³ <i>S</i> ₁	5.418(5.422)	Input	—	Input	Input	Input
³ <i>D</i> ₁	6.505(6.453)	—	—	Input	Input	—
<i>E</i> ₁	1.647(1.645)	—	—	Input	Input	—
¹ <i>D</i> ₂	-1.389(-1.377)	—	Input	Input	Input	Input
³ <i>D</i> ₂	-7.405(-7.411)	Input	Input	Input	Input	Input
³ <i>P</i> ₂	-0.2844(-0.2892)	Input	Input	Input	Input	Input
³ <i>F</i> ₂	-0.9763(-0.9698)	—	—	Input	—	—(*)
<i>E</i> ₂	1.609(1.600)	—	—	Input	—	—(*)
¹ <i>F</i> ₃	8.383(8.365)	—	—	Input	—	Input
³ <i>F</i> ₃	2.703(2.686)	—	Input	Input	Input	Input
³ <i>D</i> ₃	-0.1449(-0.1770)	Input	—	Input	Input	Input
³ <i>G</i> ₃	4.880(4.874)	—	—	Input	Input	—
<i>E</i> ₃	-9.695(-9.683)	—	—	Input	Input	—
¹ <i>G</i> ₄	-3.229(-3.210)	—	Input	Input	Input	Input
³ <i>G</i> ₄	-19.17(-19.14)	Input	Input	Input	Input	Input
³ <i>F</i> ₄	-0.01045(-0.01053)	Input	Input	Input	Input	Input
³ <i>H</i> ₄	-1.250(-1.240)	—	—	Input	—	—(*)
<i>E</i> ₄	3.609(3.586)	—	—	Input	—	—(*)
¹ <i>H</i> ₅	28.61(28.57)	—	—	Input	—	Input
³ <i>H</i> ₅	6.128(6.082)	—	Input	Input	Input	Input
³ <i>G</i> ₅	-0.0090(-0.010)	Input	—	Input	Input	Input
³ <i>I</i> ₅	10.68(10.66)	—	—	Input	Input	—
<i>E</i> ₅	-31.34(-31.29)	—	—	Input	Input	—

shifts. Due to unitarity of the S-matrix in the low energy limit, $k \rightarrow 0$ we have

$$(\mathbf{S} - \mathbf{1})_{\nu, l} = -2i\alpha_{\nu, l} k^{l'+l+1} + \dots, \quad (8)$$

with $\alpha_{\nu l}$ the (hermitian) scattering length matrix. The threshold behaviour of the SYM phases is

$$\bar{\delta}_{j-1}^{1j} \rightarrow -\bar{\alpha}_{j-1}^{1j} k^{2j-1}, \quad (9)$$

$$\bar{\delta}_{j+1}^{1j} \rightarrow -\bar{\alpha}_{j+1}^{1j} k^{2j+3}, \quad (10)$$

$$\bar{\epsilon}_j \rightarrow -\bar{\alpha}_j^{1j} k^{2j+1}. \quad (11)$$

B. Short distance behaviour

The form of the wave functions at the origin is uniquely determined by the form of the potential at short distances

(see e.g. [46, 47] for the case of one channel and [25, 26, 28, 29] for coupled channels). For the Lorentz-invariant chiral NN potential, one has

$$\mathbf{U}_{2\pi}(r) \rightarrow \frac{MC_7}{r^7},$$

which is a relativistic Van der Waals type force (see e.g. [48] for the electromagnetic case). Note that this short distance behaviour without an $1/M$ expansion is at variance with the non-relativistic $1/r^5$ and $1/r^6$ in the standard Weinberg counting based on the HB chiral expansion. In the latter, the expansion around the limit $M \rightarrow \infty$ is built in the formalism, leading to a different behavior at $r \rightarrow 0$.

For a potential diverging at the origin as an inverse power law one has

$$\mathbf{U}(r) \rightarrow \frac{MC_n}{r^n}, \quad (12)$$

with \mathbf{C}_n a matrix of generalized Van der Waals coefficients and $n > 2$. One diagonalizes the matrix \mathbf{C}_n by a constant unitary transformation, \mathbf{G} , yielding

$$M\mathbf{C}_n = \mathbf{G} \text{diag}(\pm R_1^{n-2}, \dots, \pm R_N^{n-2}) \mathbf{G}^{-1}, \quad (13)$$

with R_i constants with length dimension. The plus sign corresponds to the case with a positive eigenvalue (attractive) and the minus sign to the case of a negative eigenvalue (repulsive). Then, at short distances one has the solutions

$$\mathbf{u}(r) \rightarrow \mathbf{G} \begin{pmatrix} u_{1,\pm}(r) \\ \dots \\ u_{N,\pm}(r) \end{pmatrix}, \quad (14)$$

where for the attractive and repulsive cases one has

$$u_{i,-}(r) \rightarrow C_{i,-} \left(\frac{r}{R_i}\right)^{n/4} \sin \left[\frac{2}{n-2} \left(\frac{R_i}{r}\right)^{\frac{n}{2}-1} + \varphi_i \right], \quad (15)$$

$$u_{i,+}(r) \rightarrow C_{i,+} \left(\frac{r}{R_i}\right)^{n/4} \exp \left[-\frac{2}{n-2} \left(\frac{R_i}{r}\right)^{\frac{n}{2}-1} \right], \quad (16)$$

respectively. Here, φ_i are arbitrary short distance phases which in general depend on the energy. There are as many short distance phases as short distance attractive eigenpotentials. Orthogonality of the wave functions at the origin yield the relation

$$\sum_{i=1}^N [u_{k,i}^* u'_{p,i} - u'_{k,i}^* u_{p,i}] \Big|_{r=0} = \sum_{i=1}^A \cos(\varphi_i(k) - \varphi_i(p)), \quad (17)$$

where $A \leq N$ is the number of the short distance attractive eigenpotentials. Details on the numerical implementation of these short distance boundary conditions can be looked up in Refs. [25, 26, 28, 29].

C. Numerical parameters

The Lorentz-invariant chiral TPE potential is specified by the pion weak decay constant f_π , the nucleon axial coupling constant g_A , the nucleon mass M_N and the pion mass m_π . In addition, at the level of approximation that we are working, it is enough to consider the low energy constants c_1 , c_3 and c_4 which characterize πN scattering. The corresponding RB potential is specified by the same parameters at N³LO in the HB chiral expansion.

In our numerical calculations one takes $f_\pi = 92.4\text{MeV}$, $m_\pi = 138.03\text{MeV}$, $2\mu_{np} = M_N = 2M_p M_n / (M_p + M_n) = 938.918\text{MeV}$, $g_A = 1.29$ in the OPE piece to account for the Goldberger-Treiman discrepancy and $g_A = 1.26$ in the TPE piece of the potential. The corresponding pion

nucleon coupling constant takes then the value $g_{\pi NN} = 13.083$, according to the Nijmegen phase shift analysis of NN scattering [49]. The values of the coefficients c_1 , c_3 and c_4 used along this paper can be looked up in Table I. There we list several Sets which have been proposed in the literature [10, 20, 41, 42] as well as the one which will be used in the present work based on our analysis of deuteron properties below.

Renormalization requires fixing some low energy parameters while removing the cut-off. We take the values from the high quality potentials [43, 50] as have been obtained in Ref. [44] for the NijmII and Reid93 versions. We will use the Nijm II values for definiteness. As mentioned earlier, the number of independent parameters or counter-terms requires a study of the attractive/repulsive nature of the potential at short distances. The result of such an analysis for all channels considered in this work is summarized in table II for the different parameter sets. We also list the scattering lengths in all partial waves as determined in our previous work [44].

III. LORENTZ-INVARIANT TWO-PION EXCHANGE

A series of papers [34, 35, 36, 37] was devoted to the construction of the TPE component of the NN interaction, based on the Lorentz-invariant formulation of baryon chiral perturbation theory proposed by Becher and Leutwyler [32, 33] in their study of the πN system. These authors showed that it is possible to obtain a consistent power counting in a theory with a heavy particle without resorting to an integration of the heavy degrees of freedom and expansion around the limit of infinitely heavy baryon (HB- χ PT). The latter results can be recovered from the Lorentz-invariant formulation through an expansion in $1/m_N$. However, this procedure destroys the correct analytic behavior of the amplitude near the low energy region close to $t = 4m_\pi^2$. The underlying reason comes from the anomalous threshold of the triangle graph [32] (Fig.1) right below threshold, $t = 4m_\pi^2 - m_\pi^4/m_N^2$. In the heavy baryon limit this singularity is ignored (as it collapses to the normal threshold) and any $1/m_N$ expansion of the triangle loop around this region will fail to converge. Note that the same triangle integral also appears in the TPE potential, with two pseudo-vector vertices in one nucleon and a Weinberg-Tomozawa seagull term on the other.

In order to illustrate the problem let us consider the spectral representation of the triangle graph,

$$\gamma(t) = \frac{1}{\pi} \int_{4m_\pi^2}^{\infty} \frac{dt'}{(t' - t)} \text{Im}\gamma(t'), \quad (18)$$

where

$$\text{Im}\gamma(t') = \frac{\theta(t' - 4m_\pi^2)}{16\pi m_N \sqrt{t'}} \arctan \frac{2m_N \sqrt{t' - 4m_\pi^2}}{t' - 2m_\pi^2}. \quad (19)$$

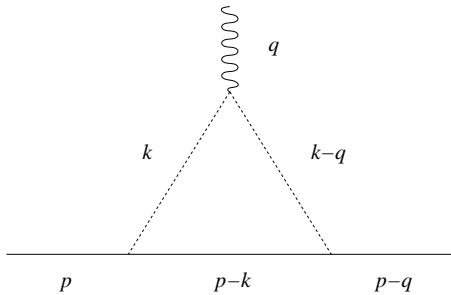


FIG. 1: The triangle diagram, which cannot be reproduced by the usual heavy baryon expansion close to $t = 4m_\pi^2$. The solid, dashed, and wiggly lines represent, respectively, the nucleon, the pions, and an external scalar source.

In HB- χ PT the argument $x = 2m_N \sqrt{t' - 4m_\pi^2} / (t' - 2m_\pi^2)$ is assumed to be of order q^{-1} , yielding the expansion $\arctan x = \pi/2 - 1/x + 1/3x^3 + \dots$. The first two terms read

$$\begin{aligned} \gamma(-q^2)|_{HB} &= \\ &= \frac{1}{16\pi^2 m_N m_\pi} \int_{4m_\pi^2}^{\infty} \frac{dt'}{(t' + q^2)} \frac{1}{\sqrt{t'}} \left[\frac{\pi}{2} - \frac{(t' - 2m_\pi^2)}{2m_N \sqrt{t' - 4m_\pi^2}} \right] \\ &= \frac{1}{16\pi^2 m_N m_\pi} \left[2\pi m_\pi A(q) + \frac{m_\pi}{m_N} \frac{(2m_\pi^2 + q^2)}{(4m_\pi^2 + q^2)} L(q) \right], \end{aligned} \quad (20)$$

where $q = |\mathbf{q}|$, and $L(q)$ and $A(q)$ are the usual HB loop functions,

$$\begin{aligned} L(q) &= \frac{\sqrt{4m_\pi^2 + q^2}}{q} \ln \frac{\sqrt{4m_\pi^2 + q^2} + q}{2m_\pi}, \\ A(q) &= \frac{1}{2q} \arctan \frac{q}{2m_\pi}. \end{aligned} \quad (21)$$

However, it does not take into consideration the case $|x| < 1$, when t' gets closer to $4m_\pi^2$. This region, where the naive heavy baryon expansion fails, is responsible for the long distance behavior of the triangle diagram, as can be seen by its representation in configuration space,

$$\begin{aligned} \Gamma(r) &= \frac{1}{\pi} \int_{4m_\pi^2}^{\infty} dt' \int \frac{d^3 q}{(2\pi)^3} e^{-i\mathbf{q}\cdot\mathbf{r}} \frac{\text{Im}\gamma(t')}{t' + q^2} \\ &= \frac{1}{4\pi^2} \int_{4m_\pi^2}^{\infty} dt' \frac{e^{-r\sqrt{t'}}}{r} \text{Im}\gamma(t'). \end{aligned} \quad (22)$$

Therefore it is clear that, in order to have a good asymptotic description of $\Gamma(r)$, one needs a decent representation for $\text{Im}\gamma(t')$ near $t' = 4m_\pi^2$. This is only possible if one takes the triangle anomalous threshold into account, which cannot be provided by current versions of the heavy baryon formalism.

The potential in configuration space is obtained through a Fourier transform of the potential in momentum space. There one faces the problem of non-localities,

i.e., terms dependent on the variable $\mathbf{z} = \mathbf{p} + \mathbf{p}'$, where \mathbf{p} and \mathbf{p}' are the initial and final CM momentum of the NN system. The relativistic loop integrals, which incorporate the dynamics of the TPE, also depend on this variable in a non-trivial way. However, phenomenologically one learns that such terms are not relevant at low energies and a Taylor expansion in \mathbf{z} is usually considered¹. In this case the Fourier transform can be carried out in an easier way (see, for instance, Refs. [51, 52]). Generically, in any spin-isospin channel and up to the considered order in the RB-expansion the potentials may be written as a function of at most second order in the total momentum operator. In this paper we take the local approximation on the radial part of the potentials and keep only up to linear terms in the operators. The remaining non-localities are fairly small all over the range of interest, which somehow justifies its exclusion and considerably simplifies our calculations².

IV. THE DEUTERON

In the pn CM system the deuteron wave function is

$$\begin{aligned} \Psi(\vec{x}) &= \frac{1}{\sqrt{4\pi r}} \left[u(r) \sigma_p \cdot \sigma_n \right. \\ &\quad \left. + \frac{w(r)}{\sqrt{8}} (3\sigma_p \cdot \hat{x} \sigma_n \cdot \hat{x} - \sigma_p \cdot \sigma_n) \right] \chi_{pn}^{sm_s} \end{aligned} \quad (23)$$

with the total spin $s = 1$ and $m_s = 0, \pm 1$ and σ_p and σ_n the Pauli matrices for the proton and the neutron respectively. The functions $u(r)$ and $w(r)$ are the reduced S- and D-wave components of the relative wave function respectively. They satisfy the coupled set of equations in the ${}^3S_1 - {}^3D_1$ channel

$$\begin{aligned} -u''(r) + U_{3S_1}(r)u(r) + U_{E_1}(r)w(r) &= -\gamma^2 u(r), \\ -w''(r) + U_{E_1}(r)u(r) + \left[U_{3D_1}(r) + \frac{6}{r^2} \right] w(r) &= -\gamma^2 w(r), \end{aligned} \quad (24)$$

with $U_{3S_1}(r)$, $U_{E_1}(r)$ and $U_{3D_1}(r)$ the corresponding matrix elements of the coupled channel potential. We solve Eq. (24) together with the asymptotic condition at infinity

$$\begin{aligned} u(r) &\rightarrow A_S e^{-\gamma r}, \\ w(r) &\rightarrow A_D e^{-\gamma r} \left(1 + \frac{3}{\gamma r} + \frac{3}{(\gamma r)^2} \right), \end{aligned} \quad (25)$$

¹ For instance, in the heavy baryon potential non-localities show up only at $O(q^4)$ ($N^3\text{LO}$).

² A rough way of estimating this in coordinate space is by acting with the operator ∇^2/m_π^2 on the local function which multiplies the variable \mathbf{z}^2 and compare with the local which multiplies the variable \mathbf{z}^0 . In the region between 0.01fm and 2fm these functions behave indeed as $1/r^7$ but the ratio between the non-local and local contribution is at the level of 1 – 5%.

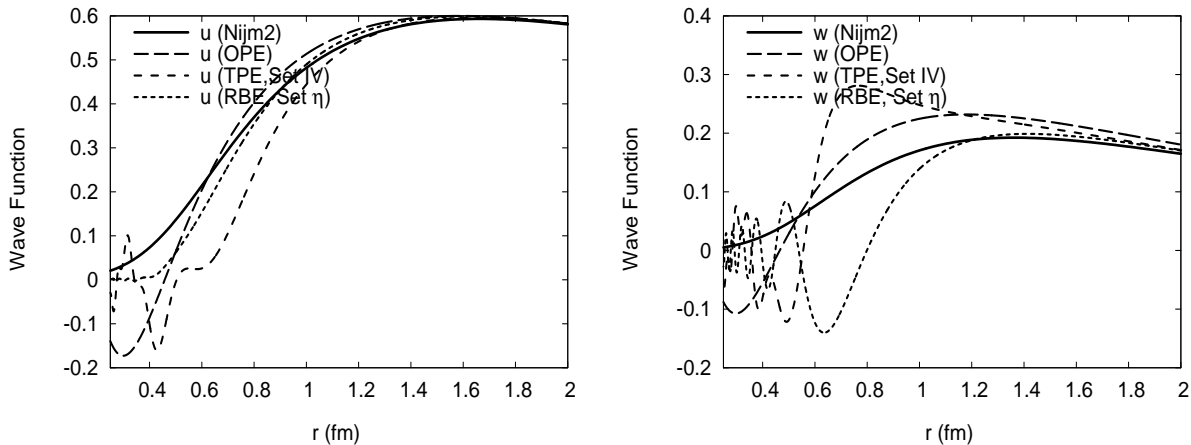


FIG. 2: RB-TPE deuteron wave functions, u (left) and w (right), as a function of the distance (in fm) compared to the HB-TPE and Nijmegen II wave functions [43]. The asymptotic normalization $u \rightarrow e^{-\gamma r}$ has been adopted and the asymptotic D/S ratio is taken $\eta = 0.0256(4)$ in the TPE case (for OPE $\eta = 0.026333$). We use the Set IV of chiral couplings and the Set η (see table I).

TABLE III: Deuteron properties for the OPE and the HB- and RB-TPE potentials. We use the non-relativistic relation $\gamma = \sqrt{2\mu_{np}B}$ with $B = 2.224575(9)$. The errors in the OPE case are estimated by changing the short distance cutoff in the range 0.1 - 0.2 fm. The errors quoted in the HB-TPE reflect the uncertainty in the non-potential parameters γ , η only. The errors quoted in the RB-TPE are estimated as in the OPE case, but changing the cutoff in the range 0.3 - 0.4 fm. The entry Exp. stands for Experimental and/or recommended values and can be traced from Ref. [53].

Set	$\gamma(\text{fm}^{-1})$	η	$A_S(\text{fm}^{-1/2})$	$r_d(\text{fm})$	$Q_d(\text{fm}^2)$	P_D	$\langle r^{-1} \rangle(\text{fm}^{-1})$	$\langle r^{-2} \rangle(\text{fm}^{-2})$	$\langle r^{-3} \rangle(\text{fm}^{-3})$
OPE	Input	0.02634	0.8681(1)	1.9351(5)	0.2762(1)	7.88(1)%	0.4861(10)	0.434(3)	∞
HB Set IV	Input	Input	0.884(4)	1.967(6)	0.276(3)	8(1)%	0.447(5)	0.284(8)	0.276(13)
RBE Set IV	Input	0.03198(3)	0.8226(5)	1.8526(10)	0.3087(2)	22.99(13) %	0.5054(15)	0.360(4)	0.333(13)
RBE Set η	Input	0.02566(1)	0.88426(2)	1.96776(1)	0.2749(1)	5.59(1) %	0.4438(3)	0.2714(7)	0.215(3)
NijmII	0.231605	0.02521	0.8845(8)	1.9675	0.2707	5.635%	0.4502	0.2868	∞
Reid93	0.231605	0.02514	0.8845(8)	1.9686	0.2703	5.699%	0.4515	0.2924	∞
Exp.	0.231605	0.0256(4)	0.8846(9)	1.971(6)	0.2859(3)	5.67(4)%	-	-	-

where $\gamma = \sqrt{MB}$ is the deuteron wave number (B is the deuteron binding energy), A_S is the s-wave normalization factor determined from the condition

$$\int_0^\infty dr [u(r)^2 + w(r)^2] = 1, \quad (26)$$

and the asymptotic D/S ratio parameter is defined by $\eta = A_D/A_S$. As we have mentioned already the RB-TPE potential displays a relativistic $1/r^7$ Van der Waals singularity at the origin. Thus, the discussion on whether or not the deuteron parameters γ and η can be fixed independently on the potential depends on the short distance behaviour of the eigenvalues of the coupled channel potential matrix. As discussed in Ref. [25, 26, 28, 29] also for the bound state case the number of independent parameters coincides with the number of negative (attractive) eigenpotentials at short distances. In the RB-TPE potential we are using here [34, 35, 36] we have only one independent parameter (see table II) which we take to be γ or, equivalently, the deuteron binding energy. With

such a choice η becomes a prediction in contrast to the HB-TPE where η is an input. The outgoing deuteron wave functions are depicted in Fig. 2 for the RB-TPE potential and compared to the HB-TPE one.

Let us analyze in more detail the cut-off dependence of observables in the present RB-TPE potential. Given the fact that in the ${}^3S_1 - {}^3D_1$ coupled channel we have one attractive and one repulsive eigenpotential at short distances we may borrow from the previous discussion on OPE [25] where we refer for further details. The practical way of introducing in this case a short distance cut-off r_c which selects the regular solution at the origin is by appropriately choosing the auxiliary boundary condition at the point $r = r_c$ among many possible choices compatible with self-adjointness [25]. The precise choice may provide smoother limits and hence better convergence properties in the pre-asymptotic region. Actually, as we show in Appendix A, we can estimate the size of the finite cut-off corrections in deuteron observables and

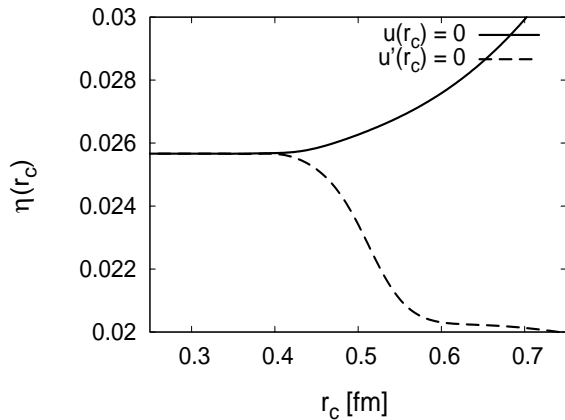


FIG. 3: Cut-off dependence of the asymptotic D/S ratio of the deuteron wave function, η , as a function of the short distance cut-off r_c (in fm) for the RB-TPE potential for the auxiliary boundary conditions $u(r_c) = 0$ and $u'(r_c) = 0$. We use the Set η of chiral couplings and the Set η (see table I) designed to reproduce the experimental value $\eta = 0.0256(4)$ in the limit $r_c \rightarrow 0$. The convergence towards the renormalized value is $\eta(r_c) - \eta(0) \sim \exp[-2/5(R_+/r_c)^{5/2}]$ up to oscillations (see main text).

hence their convergence rate towards the corresponding renormalized values. The result is that up to some oscillations the convergence towards the renormalized value is exponential as $r_c \rightarrow 0$, i.e. the convergence towards the renormalized value is $\eta(r_c) - \eta(0) \sim \exp[-4/5(R_+/r_c)^{5/2}]$ for the RB-TPE potential ($\sim 1/r^7$) as compared to $\eta(r_c) - \eta(0) \sim \exp[-2(R_+/r_c)^{1/2}]$ for the OPE potential ($\sim 1/r^3$). Here R_+ is a characteristic short distance scale of the corresponding repulsive eigenpotentials. The analysis of Appendix A also shows that, generally, the more singular the potential the faster the convergence.

For illustration purposes we show in Fig. 3 the calculated asymptotic D/S ratio of the deuteron wave function, η , as a function of the short distance cut-off r_c (in fm) for the RB-TPE potential when the auxiliary boundary conditions $u(r_c) = 0$ and $u'(r_c) = 0$ are considered. Note the clear and coincident plateau below $r_c = 0.4$ fm for both boundary conditions following a relatively rapid variation above this region³. As mentioned above, this is a typical feature of a coupled channel singular potential with one attractive and one repulsive eigenpotential which extends to all other deuteron properties. Actually, the situation strongly resembles the previously studied OPE potential which has a softer $1/r^3$ singularity at the

origin [25]; the main difference is that for OPE stability takes place at a shorter scale, $r_c = 0.2$ fm, than in RB-TPE potential. In the present context it is also helpful to remind that a short distance cut-off radius and a sharp momentum cut-off are inverse proportional to each other, $r_c = \pi/(2\Lambda)$ [54] (the numerical coefficient depends on the particular regularization). Thus plotting observables as a function of r_c enhances the finite cut-off changes while long plateaus could be observed instead as functions of Λ . Actually, halving the short distance cut-off corresponds to doubling the momentum space cut-off. For instance, in RB (Set- η) the range $r_c = 0.3 - 0.4$ fm corresponds to the range $\Lambda = 780 - 1030$ MeV where observables such as η change less than 0.01%. Pinning down this error bar would be harder if the sharp or other momentum space cut-off was used.

Our results for several deuteron properties are shown in table III and compared to the corresponding HB-TPE considered in our previous work [25, 26, 28, 29]. Some remarks concerning the errors quoted in table III are in order. We provide the largest source of error in the calculation which we are able to quantify. Since we aim at renormalized results, we stop whenever the change of the cut-off causes no significant variation within a prescribed accuracy, which we take to be about an order of magnitude higher than the typical experimental or recommended value uncertainty. Thus, the cut-off range is not necessarily the same in all cases. In general terms, the more singular the potential at short distance, the faster the convergence of the result towards the renormalized limit (see e.g. Appendix A). Thus, the toughest case is OPE, where we only have $1/r^3$ singularity. Convergence in this case is the slowest, therefore shorter cut-offs $r_c = 0.1 - 0.2$ fm are needed.

The value we obtain for η for the parameter Sets of table I is slightly different from the experimental one, making the comparison with the HB-TPE case [26], where η was a free parameter (two attractive short distance eigenpotentials), a bit misleading. In order to obtain an accurate value of η it was necessary to readjust the low energy parameters c_3 and c_4 to the values $c_3 = -3.8 \text{ GeV}^{-1}$ and $c_4 = 4.5 \text{ GeV}^{-1}$, indeed, very similar to the values proposed by other authors [10, 20, 41, 42] (see table I). Actually, once we have reproduced η we see a general and slight improvement in accuracy when going from the HB-TPE (where η is a free parameter) of our previous work [26] to the present RB-TPE calculation (where η is predicted). Basically, RB-TPE produces a sharp prediction for η (with eventually no errors), whereas HB-TPE does not predict η , so its 1% experimental uncertainty propagates to other deuteron observables at about a similar 1% level, which is still comparable or larger than the error in the quoted experimental or recommended values. The conclusion in Ref. [26] was that agreement was partly achieved because of this fuzziness in the theoretical predictions. Of course, one should not overstress the possible accuracy of the present results as regards the systematic errors; the main point of our calculation is to

³ Other auxiliary boundary conditions such as $w(r_c) = 0$ or $w'(r_c) = 0$ not shown in the figure make the oscillations deduced in Appendix A more visible, but the plateau region takes place also below $r_c = 0.4$ fm and yields an identical numerical result as with $u(r_c) = 0$ and $u'(r_c) = 0$.

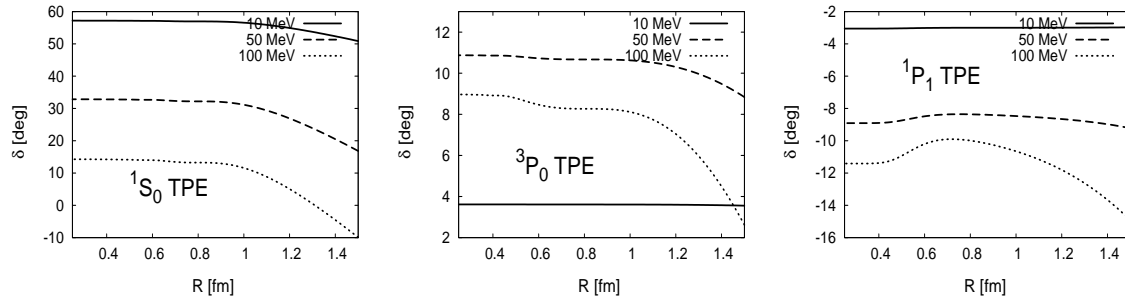


FIG. 4: Relativistic Baryon expansion (RBE) np phase shifts in the 1S_0 , 3P_0 and 1P_1 channels as a function the short distance cut-off radius r_c for the fixed laboratory energies $T_L = 10, 50, 100\text{MeV}$.

provide the general picture when more complete asymptotic TPE effects are correctly taken into account.

V. PHASE SHIFTS

We come to the calculation of the np phase shifts. In practice, this requires a careful wave by wave study of the renormalized limit. As can be seen in table II, all coupled triplet channels have one attractive and one repulsive short distance $1/r^7$ eigenpotential. On the other hand, almost all singlet and uncoupled triplet channels develop an attractive $1/r^7$ singularity at short distances (sometimes depending on the parameter values). The only exceptions we found are the 1P_1 and 3P_0 channels, the latter depending on the precise values of the $c_{1,3,4}$ constants of the chiral potential. This fact determines not only the number of counterterms, but also the convergence pattern towards the renormalized result. It reaches stability for cut-offs ranging in the region $r_c = 0.3 - 0.5\text{fm}$, depending on the particular partial wave and also on the energy (see the discussion in the previous section IV and Appendix A). Phase shifts in coupled channels with one repulsive singular component have been computed with either auxiliary boundary conditions $u_{0,j,l=j-1}(r_c) = 0$ and $u'_{0,j,l=j-1}(r_c) = 0$ for zero energy states and subsequent orthogonalization of the finite energy states by using a complementary boundary condition as described in detail in Ref. [25] for the OPE case. It is important to realize that even though renormalization requires in principle to pursue the mathematical limit $r_c \rightarrow 0$, convergence is achieved in practice by length scales which are not unrealistically small and in fact are rather reasonable. This can be seen in Fig. 4 where, for illustration purposes, some selected low phases are depicted as a function of the short distance cut-off for fixed laboratory energy values. As one generally expects smaller values of r_c are needed as the energy is increased. The approach towards the renormalized value for any partial wave depends on the attractive/repulsive character of the singular potential at short distances. So, the 1S_0 and 3P_0 channels are purely attractive and hence the finite cut-off corrections

are $\mathcal{O}(r_c^{\frac{7}{2}+1})$ up to oscillations [40]. On the other hand, the 1P_1 channel provides a repulsive case and hence finite cut-off corrections are $\mathcal{O}(e^{-r_c^{-\frac{5}{2}}})$. We remind that the smallest de Broglie wavelength probed in NN interaction below pion production threshold is $\lambda \sim 0.5\text{fm}$. Thus, the RB-potential and the present renormalization construction also implement the desirable *a priori* requirement that short distance details are indeed irrelevant for the description of low energy properties.

In Figs. 5 and 6 we present the np (SYM-nuclear bar) renormalized phase shifts for the total angular momentum $j = 0, 1, 2, 3, 4, 5$ for Spin Singlet and Uncoupled Spin Triplet and Coupled Spin Triplet channels respectively. There we compare the relativistic baryon expansion (RBE) and the heavy baryon expansion (HBE) as a function of the LAB energy compared to the Nijmegen partial wave analysis [43, 50]. For definiteness we use the chiral constants c_1 , c_3 and c_4 of Ref. [20] (Set IV), which already provided a good description of deuteron properties after renormalization [26] at NNLO. This choice allows a more straightforward comparison to the N³LO calculation of Ref. [20] with finite cut-offs. We also compare with the Set η which takes to the same value of c_1 and the readjusted values $c_3 = -3.8\text{GeV}^{-1}$ and $c_4 = 4.5\text{GeV}^{-1}$ based on our improved description of the deuteron in Sec. IV. Unless otherwise stated, the needed low energy parameters for these figures are *always* taken to be those of Ref. [44] for the NijmII potential (see Table II). As can be clearly seen, the RB-TPE with this Set- η not only improves deuteron properties but also the phase shifts all over. Again, one should not overemphasize this agreement, but it is rewarding to see that there is a general trend to stability and improvement in some channels (such as $^1D_2, ^3P_1, ^3P_0$) when the RB-TPE potential is considered, while the quality of description is not worsened in other channels. At the same time one should stress, however, that generally speaking this potential needs much less counter-terms as the corresponding HB counterpart (about a half). Actually, in the Lorentz-invariant potential case one has at most one free parameter for channel as compared to the three parameters for channels in the coupled triplets. This is due

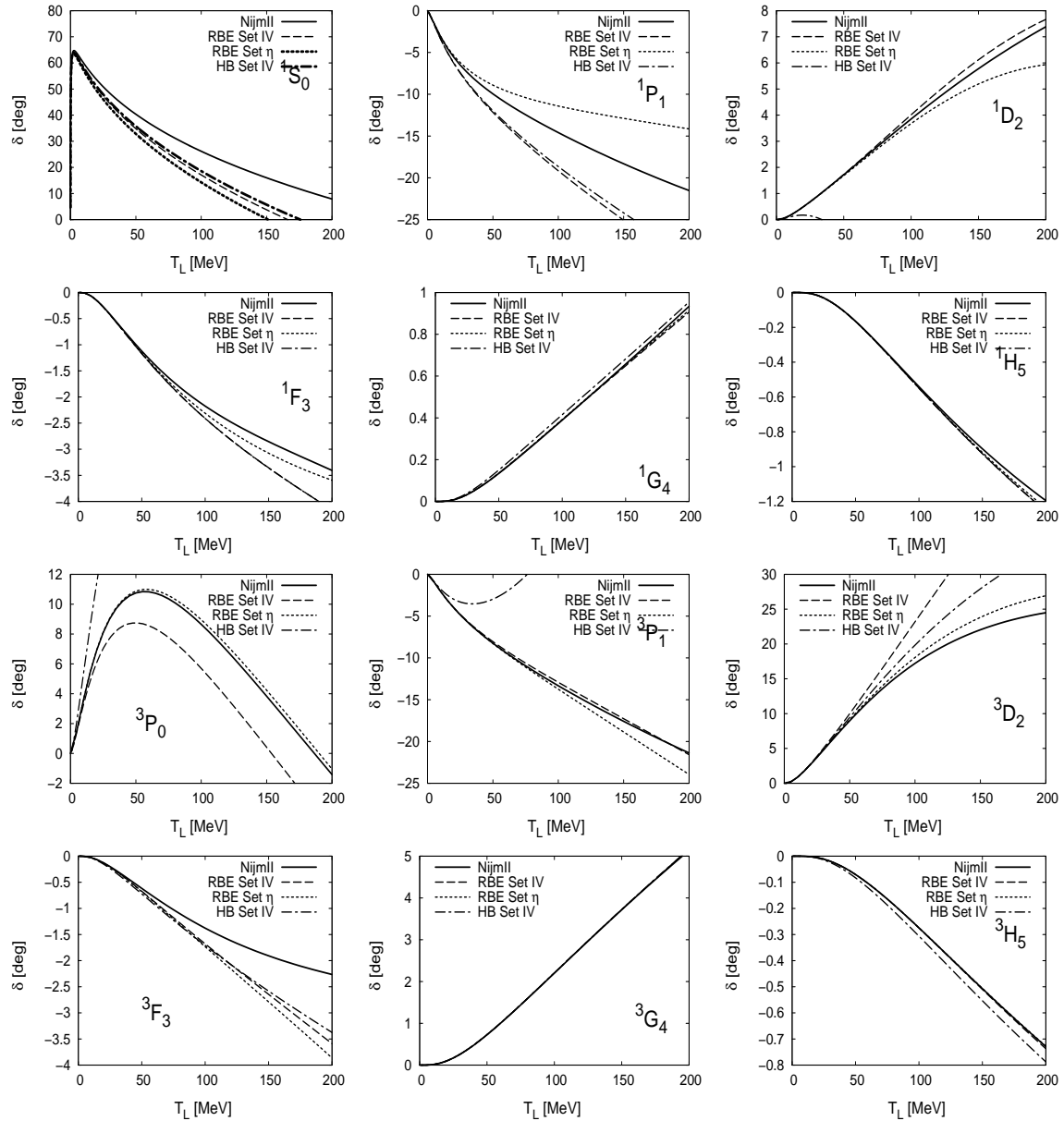


FIG. 5: np (SYM-nuclear bar) Spin Singlet and Uncoupled Spin Triplet phase shifts for the total angular momentum $j = 0, 1, 2, 3, 4, 5$ for relativistic baryon expansion (RBE) and for the heavy baryon expansion (HBE) as a function of as a function of the LAB energy compared to the Nijmegen partial wave analysis [43, 50].

to the attractive-repulsive short distance character of the coupled channel RB-TPE as compared to the attractive-attractive HB-TPE potential in these coupled channels. Again, we remind that the RB-TPE provides the correct analytic behavior of the exchange of two pions at large distances when Δ and other excitations are not explicitly considered.

VI. CONCLUSIONS

In the present paper we have analyzed the renormalization of all partial waves for NN scattering and the bound deuteron state for the Chiral Two Pion Exchange Potential computed in a relativistic baryon Expansion. Our main motivation has been to consider a potential where the asymptotic TPE effects are consistently taken care of. This gives us some confidence that long distance physics is faithfully represented by a common exponential fall-off factor $e^{-2m_\pi r}$. At the level of calculation considered

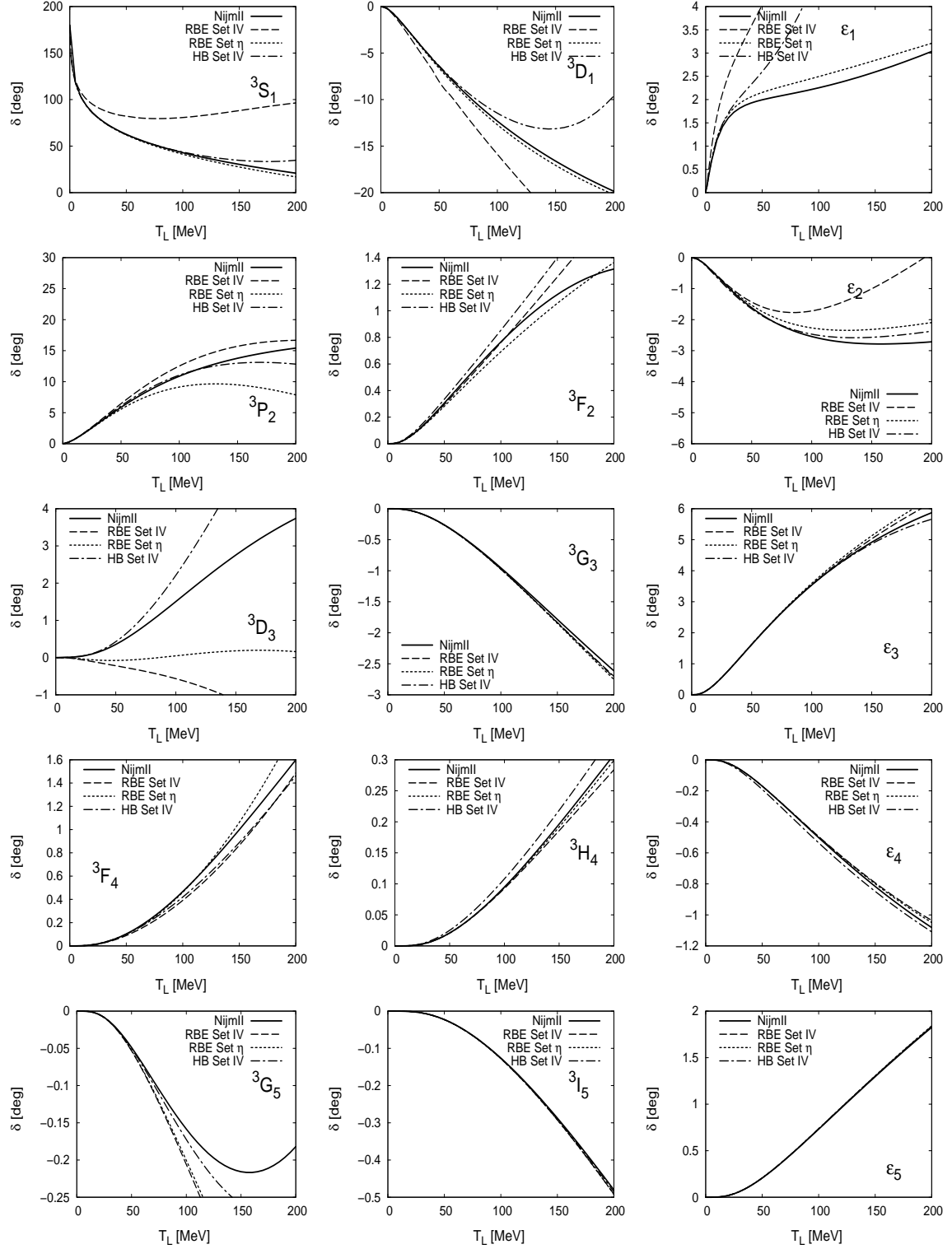


FIG. 6: np (SYM-nuclear bar) Coupled Spin Triplet Phase shifts for the total angular momentum $j = 0, 1, 2, 3, 4, 5$ for relativistic baryon expansion (RBE) and for the heavy baryon expansion (HBE) as a function of as a function of the LAB energy compared to the Nijmegen partial wave analysis [43, 50].

here Δ and other excitations are not explicitly taken into account; within a relativistic baryon expansion the contribution of this degree of freedom to the NN potential has never been computed. In addition, in the relativistic baryon expansion there appear non-local terms in the potential which involve the sum of initial and final momentum space operators which fortunately turn out to be rather small all over the range as compared to the local contributions to the potential. This simplifies the analysis tremendously since standard coordinate space methods can be used to solve the non-perturbative scattering problem and deuteron bound state and their subsequent and necessary renormalization. As we have repeatedly stressed along the paper this Lorentz-invariant potential presents a $1/r^7$ singularity at the origin which demands renormalization in order to get a finite and unique result when the TPE potential is assumed to be valid all over the range from the origin to infinity. This can be done by introducing a number of (potential independent) counter-terms and consequently physical renormalization conditions must be specified. In practice they are fixed to the values of threshold parameters, mainly scattering lengths at zero energy. Actually, we have noted that the number of necessary counter-terms is drastically reduced when the Lorentz-invariant baryon potential is compared to the heavy baryon expanded TPE potential, while both potentials are specified by the same parameters. Thus, less input is needed to predict the NN phase-shifts. Although the precise number of counter-terms depends on the parameters of the potential we find that, typically, for the channels with total angular momentum $j = 0$ to 5 we need 13 in the Lorentz-invariant case as compared to about 27 in the HB potential. Actually, it is noteworthy that with about a half of the counter-terms the overall agreement is improved. This is particularly striking in the 3P_0 and the ${}^3S_1 - {}^3D_1$ (deuteron) channels. In other channels the improvement is moderate, indicating missing shorter range contributions to Eq. (1). Although a deeper understanding on why this dramatic reduction of the number of counter-terms happens would very helpful, and we have not attempted a large scale fit, it is very rewarding that the implementation of the correct and fairly complete long range physics deduced from One and Two Pion Exchange in conjunction with the requirement of renormalizability provides a rather reasonable description of the NN scattering data below pion production threshold.

Acknowledgments

We would like to thank the hospitality of the European Center for Theoretical Studies on Nuclear Physics and Related Areas (ECT*) in Trento, where this work was initiated. M.P.V. also thanks W. Broniowski and P. Bożek for their kind hospitality in Krakow where part of this work has been carried out.

The work of M.P.V. and E.R.A. is supported in part by funds provided by the Spanish DGI and FEDER funds with grant no. FIS2005-00810, Junta de Andalucía grants no. FQM225-05, EU Integrated Infrastructure Initiative Hadron Physics Project contract no. RII3-CT-2004-506078. The work of R.H. was supported by DOE Contract No.DE-AC05-06OR23177, under which SURA operates the Thomas Jefferson National Accelerator Facility, and by the BMBF under contract number 06BN411.

APPENDIX A: ANALYTICAL DETERMINATION OF FINITE CUT-OFF CORRECTIONS

In this appendix we determine the finite cut-off corrections to renormalized deuteron properties when the the two coupled channel potential is so that there is one attractive and one repulsive short distance eigenpotential. This is the case of OPE and RB-TPE potentials discussed in this paper. In this case it is simplest to discuss the auxiliary boundary condition

$$u(r_c) = 0 \quad (\text{A1})$$

The analysis of other auxiliary boundary conditions such as $u'(r_c) = 0$ which has actually been used in the numerical calculations is a bit messier but the final conclusion is essentially the same as with Eq. (A1).

From the superposition principle of boundary conditions we may write

$$\begin{aligned} u(r) &= u_S(r) + \eta u_D(r), \\ w(r) &= w_S(r) + \eta w_D(r), \end{aligned} \quad (\text{A2})$$

where $(u_S(r), w_S(r))$ and $(u_D(r), w_D(r))$ solve the deuteron problem, Eq. (24), with the long distance boundary conditions Eq. (25) when taking $(A_S, A_D) = (1, 0)$ and $(A_S, A_D) = (0, 1)$ respectively. On the other hand, at short distances the coupled channel potential is diagonalized by an orthogonal transformation

$$\mathbf{G} = \begin{pmatrix} \cos \theta & \sin \theta \\ -\sin \theta & \cos \theta \end{pmatrix} \quad (\text{A3})$$

where the mixing angle θ depends on the parameters of the potential only. For instance, for OPE one has $\cos \theta = -1/\sqrt{3}$, see Ref. [25]. The reduced potential behaves as

$$\mathbf{U}(r) \rightarrow \frac{1}{r^n} \mathbf{G} \begin{pmatrix} +R_+^{n-2} & 0 \\ 0 & -R_-^{n-2} \end{pmatrix} \mathbf{G}^{-1} \quad (\text{A4})$$

where R_+ and R_- are the Van der Waals length scales associated to the repulsive and attractive channels respectively. Defining the general short distance solutions of the decoupled problems

$$\begin{aligned}
v_{i,+}(r) &= \left(\frac{r}{R_+}\right)^{n/4} \left\{ a_{i,+} \exp \left[-\frac{2}{n-2} \left(\frac{R_+}{r}\right)^{\frac{n-2}{2}} \right] + b_{i,+} \exp \left[+\frac{2}{n-2} \left(\frac{R_+}{r}\right)^{\frac{n-2}{2}} \right] \right\} \\
v_{i,-}(r) &= \left(\frac{r}{R_-}\right)^{n/4} c_{i,-} \sin \left[\frac{2}{n-2} \left(\frac{R_-}{r}\right)^{\frac{n-2}{2}} + \varphi_i \right]
\end{aligned} \tag{A5}$$

where $i = S, D$ and $a_{i,+}$, $b_{i,+}$, $c_{i,-}$, φ_i are fixed constants which depend on the potential only and may be determined by integrating in from long distances the asymptotic wave functions ($u_S(r), w_S(r)$) and ($u_D(r), w_D(r)$). We remind that $n = 7$ for the RB-TPE potential while $n = 3$ for the OPE potential. Note that we must include here also the diverging exponential at the origin for the repulsive eigenpotential. The solutions at short distances behave as

$$\begin{pmatrix} u_i(r) \\ w_i(r) \end{pmatrix} \rightarrow \begin{pmatrix} \cos \theta & \sin \theta \\ -\sin \theta & \cos \theta \end{pmatrix} \begin{pmatrix} v_{i,+}(r) \\ v_{i,-}(r) \end{pmatrix} \tag{A6}$$

where $i = S, D$. Thus, using the short distance boundary condition, Eq. (A1) which selects the regular solution at the origin and eventually kills the diverging exponentials

when $r_c \rightarrow 0$, and gathering all subsequent equations we get

$$\begin{aligned}
\eta(r_c) &= -\frac{u_S(r_c)}{u_D(r_c)} \\
&\rightarrow \frac{\cos \theta v_{S,+}(r_c) + \sin \theta v_{S,-}(r_c)}{\cos \theta v_{D,+}(r_c) + \sin \theta v_{D,-}(r_c)}
\end{aligned} \tag{A7}$$

The limiting value is controlled by the short distance diverging exponentials in Eq. (A5) and is given by

$$\eta(0) = -\frac{b_{S,+}}{b_{D,+}} \tag{A8}$$

Deviations from this value for small cut-offs r_c can be directly determined from Eq. (A5) yielding

$$\frac{\eta(r_c)}{\eta(0)} = 1 + \tan \theta \left(\frac{R_+}{R_-}\right)^{\frac{n}{4}} \left[\frac{c_{S,-}}{b_{S,+}} - \frac{c_{D,-}}{b_{D,+}} \right] \exp \left[-\frac{2}{n-2} \left(\frac{R_+}{r_c}\right)^{\frac{n-2}{2}} \right] \sin \left[\frac{2}{n-2} \left(\frac{R_-}{r_c}\right)^{\frac{n-2}{2}} + \varphi_i \right] + \dots \tag{A9}$$

showing that, up to oscillations, finite cut-off corrections in the deuteron are $\mathcal{O}(e^{-r_c^{-\frac{1}{2}}})$ for OPE and $\mathcal{O}(e^{-r_c^{-\frac{5}{2}}})$ for RB-TPE. The generalization to other auxiliary boundary conditions and other deuteron properties is straightforward with identical result in the order of finite cut-off effects.

The case of scattering states is more tedious and will not be discussed in detail here but can also be analyzed

with a combination of the coupled channel formulas of Ref. [40] (see Sect. V of that paper) and the bound state results of the present appendix. Finite cut-off effects for the S-matrix scale similarly as in the bound state case, i.e. up to oscillations they are $\mathcal{O}(e^{-r_c^{-\frac{1}{2}}})$ for OPE and $\mathcal{O}(e^{-r_c^{-\frac{5}{2}}})$ for RB-TPE.

-
- [1] G. Brown and A. D. Jackson, *The Nucleon-Nucleon Interaction* (North-Holland Publishing Company, Amsterdam, 1976).
 - [2] R. Machleidt, K. Holinde, and C. Elster, Phys. Rept. **149**, 1 (1987).
 - [3] S. Weinberg, Phys. Lett. **B251**, 288 (1990).
 - [4] C. Ordonez and U. van Kolck, Phys. Lett. **B291**, 459 (1992).
 - [5] S. Weinberg, Nucl. Phys. **B363**, 3 (1991).
 - [6] C. Ordonez, L. Ray, and U. van Kolck, Phys. Rev. **C53**, 2086 (1996), hep-ph/9511380.
 - [7] T. A. Rijken and V. G. J. Stoks, Phys. Rev. **C54**, 2851 (1996), nucl-th/9509029.
 - [8] N. Kaiser, R. Brockmann, and W. Weise, Nucl. Phys. **A625**, 758 (1997), nucl-th/9706045.
 - [9] J. L. Friar, Phys. Rev. **C60**, 034002 (1999), nucl-th/9901082.
 - [10] M. C. M. Rentmeester, R. G. E. Timmermans, J. L. Friar, and J. J. de Swart, Phys. Rev. Lett. **82**, 4992 (1999), nucl-th/9901054.
 - [11] D. R. Entem and R. Machleidt, Phys. Rev. **C66**, 014002 (2002), nucl-th/0202039.

- [12] P. F. Bedaque and U. van Kolck, *Ann. Rev. Nucl. Part. Sci.* **52**, 339 (2002), nucl-th/0203055.
- [13] D. R. Phillips, *Czech. J. Phys.* **52**, B49 (2002), nucl-th/0203040.
- [14] E. Epelbaum, *Prog. Part. Nucl. Phys.* **57**, 654 (2006), nucl-th/0509032.
- [15] M. Rho (2006), nucl-th/0610003.
- [16] E. Ruiz Arriola and M. Pavon Valderrama (2006), nucl-th/0609080.
- [17] E. Epelbaum, W. Gloeckle, and U.-G. Meissner, *Nucl. Phys.* **A671**, 295 (2000), nucl-th/9910064.
- [18] D. R. Entem and R. Machleidt, *Phys. Lett.* **B524**, 93 (2002), nucl-th/0108057.
- [19] S. R. Beane, P. F. Bedaque, M. J. Savage, and U. van Kolck, *Nucl. Phys.* **A700**, 377 (2002), nucl-th/0104030.
- [20] D. R. Entem and R. Machleidt, *Phys. Rev.* **C68**, 041001 (2003), nucl-th/0304018.
- [21] E. Epelbaum, W. Glockle, and U.-G. Meissner, *Nucl. Phys.* **A747**, 362 (2005), nucl-th/0405048.
- [22] M. Pavon Valderrama and E. Ruiz Arriola, *Phys. Rev.* **C70**, 044006 (2004), nucl-th/0405057.
- [23] M. C. Birse and J. A. McGovern, *Phys. Rev.* **C70**, 054002 (2004), nucl-th/0307050.
- [24] A. Nogga, R. G. E. Timmermans, and U. van Kolck, *Phys. Rev.* **C72**, 054006 (2005), nucl-th/0506005.
- [25] M. Pavon Valderrama and E. Ruiz Arriola, *Phys. Rev.* **C72**, 054002 (2005), nucl-th/0504067.
- [26] M. Pavon Valderrama and E. Ruiz Arriola, *Phys. Rev.* **C74**, 054001 (2006), nucl-th/0506047.
- [27] M. C. Birse, *Phys. Rev.* **C74**, 014003 (2006), nucl-th/0507077.
- [28] M. Pavon Valderrama and E. Ruiz Arriola, *Phys. Rev.* **C74**, 064004 (2006), nucl-th/0507075.
- [29] M. Pavon Valderrama and E. Ruiz Arriola, *Phys. Rev.* **C75**, 059905(E) (2007).
- [30] E. Epelbaum and U. G. Meissner (2006), nucl-th/0609037.
- [31] M. C. Birse (2007), arXiv:0706.0984 [nucl-th].
- [32] T. Becher and H. Leutwyler, *Eur. Phys. J.* **C9**, 643 (1999), hep-ph/9901384.
- [33] T. Becher and H. Leutwyler, *JHEP* **06**, 017 (2001), hep-ph/0103263.
- [34] R. Higa and M. R. Robilotta, *Phys. Rev.* **C68**, 024004 (2003), nucl-th/0304025.
- [35] R. Higa, M. R. Robilotta, and C. A. da Rocha, *Phys. Rev.* **C69**, 034009 (2004), nucl-th/0310011.
- [36] R. Higa (2004), nucl-th/0411046.
- [37] R. Higa, M. R. Robilotta, and C. A. da Rocha (2005), nucl-th/0501076.
- [38] N. Kaiser, S. Gerstendorfer, and W. Weise, *Nucl. Phys.* **A637**, 395 (1998), nucl-th/9802071.
- [39] S. R. Beane et al., *Phys. Rev.* **A64**, 042103 (2001), quant-ph/0010073.
- [40] M. Pavon Valderrama and E. Ruiz Arriola (2007), arXiv:0705.2952 [nucl-th].
- [41] P. Buettiker and U.-G. Meissner, *Nucl. Phys.* **A668**, 97 (2000), hep-ph/9908247.
- [42] E. Epelbaum, W. Gloeckle, and U.-G. Meissner, *Eur. Phys. J.* **A19**, 401 (2004), nucl-th/0308010.
- [43] V. G. J. Stoks, R. A. M. Klomp, C. P. F. Terheggen, and J. J. de Swart, *Phys. Rev.* **C49**, 2950 (1994), nucl-th/9406039.
- [44] M. Pavon Valderrama and E. Ruiz Arriola, *Phys. Rev.* **C72**, 044007 (2005).
- [45] H. P. Stapp, T. J. Ypsilantis, and N. Metropolis, *Phys. Rev.* **105**, 302 (1957).
- [46] K. M. Case, *Phys. Rev.* **80**, 797 (1950).
- [47] W. Frank, D. J. Land, and R. M. Spector, *Rev. Mod. Phys.* **43**, 36 (1971).
- [48] G. Feinberg, J. Sucher, and C. K. Au, *Phys. Rept.* **180**, 83 (1989).
- [49] J. J. de Swart, M. C. M. Rentmeester, and R. G. E. Timmermans, *PiN Newslett.* **13**, 96 (1997), nucl-th/9802084.
- [50] V. G. J. Stoks, R. A. M. Kompl, M. C. M. Rentmeester, and J. J. de Swart, *Phys. Rev.* **C48**, 792 (1993).
- [51] M. H. Partovi and E. L. Lomon, *Phys. Rev.* **D2**, 1999 (1970).
- [52] N. Hoshizaki and S. Machida, *Prog. Theor. Phys.* **24**, 1325 (1960).
- [53] J. J. de Swart, C. P. F. Terheggen, and V. G. J. Stoks (1995), nucl-th/9509032.
- [54] M. Pavon Valderrama and E. Ruiz Arriola (2004), nucl-th/0410020.